$(R'_{max} - R'_{min}) < 0.1$ (i.e., $R' \simeq R'_{min}$) or $0 \leq (R'_{max} - R')/(R'_{max} - R'_{min}) < 0.1$ (i.e., $R' \simeq R'_{max}$). The sign of the counts for materials such as silicon, for which optical path length increases with temperature, is shown in Table 1. The results of this algorithm are shown in Fig. 3 for a simulated reflectance trace. The accuracy of such an algorithm could be within 1/4 of an optical fringe. This corresponds to ≈1.5°C using a 640-μm-thick Si wafer as an example.

In summary, we have used the wavelength modulation capability of the DFB laser diode for interferometric thermometry measurements in which the magnitude and direction of temperature change can be determined.

1. M. Luckiesh, L. L. Holladay, and R. H. Sinden, J. Franklin Inst. **194**, 251 (1922).
2. F. C. Nix and D. MacNair, Rev. Sci. Instrum. **12**, 66 (1941).
3. K. L. Saenger, R. A. Roy, J. Gupta, J. P. Doyle, and J. J. Cuomo, "Laser Interferometric Temperature Measurement of Heated Substrates Used for High T_c Superconductor Deposition," to be published in *Symposium Proceedings M* (Materials Research Society, Pittsburgh, Pa., 1990).
4. K. L. Saenger and J. Gupta, "Laser Interferometric Thermometry for Substrate Temperature Measurement," accepted for Appl. Opt. (January, 1990).
5. V. M. Donnelly and J. A. McCaulley, J. Vac. Sci. Technol. A **8**, 84 (1990).
6. K. L. Saenger, unpublished results.
7. H. Sankur and W. Gunning, Appl. Phys. Lett. **56**, 2651 (1990).

2:15 pm

CThK4 Laser vision sensor for disaster-prevention robot

Osamu Yamada, Minoru Kimura, Hidemi Takahashi, and Hiroshi Naitoh
Matsushita Research Institute Tokyo, Inc., 3-10-1 Higashimita, Tama-ku, Kawasaki 214, Japan

One of the roles of disaster-prevention robots in the event of a disaster is to discover what is happening and to perform the counter action in circumstances where the visibility is reduced to zero by flame and smoke. It was desirable to develop a vision sensor for disaster-prevention robots so they can acquire 3D-information where ordinary vision sensors are impossible to use.[1]

We have developed a range-measuring 3D-vision sensor by a laser-radar system using a CO_2 laser with a wavelength of 10.6 μm capable of propagating through an environment of smoke, dust, and mist.[2]

The configuration of the laser vision sensor is shown in Fig. 1. The CO_2 laser beam is amplitude-modulated by electro-optic light modulator (EOM) sinusoidally and irradiated onto a target with a 2D-scanner. The reflected laser signals are received by an infrared detector (HgCdTe) through the same scanner. To eliminate radiant light from a flame and to receive only the laser light, a narrow-band optical filter is installed in front of the detector. In the image processing unit, an image is obtained in proportion to the intensity of the signals, and a range image is obtained by the phase difference between the signals and the reference wave. Although the frame rate is limited to eight 128 X 128 images per second because of the performance of the 2D-scanner, the real pixel rate is 400 KHz, and a high range resolution of 10 cm is achieved in an indoor environment.

This vision sensor has been tested in a laboratory simulation of disaster environments, flame, smoke,[3] dust, and mist, separately and in conjunction. The laser propagation characteristics in the flame environment using 40 MHz amplitude-modulation are shown in Fig. 2.

It has been confirmed that more than 50% of the CO_2 laser beam can propagate through a propane gas flame of W50 cm x D50 cm x H100 cm burning at a rate of 120 l/min, through which nothing can be seen with the naked eye. The fluctuation and shift of the detected phase difference are kept under 0.5 and 4 degrees respectively. It was also turned out that deflection of laser light by a flame is less than 3 pixels in the image of targets at a range of 30 m.

A range image in an indoor environment is shown in Fig. 3(a) in which the targets are a stainless steel valve and a polystyrene snowman and the background is polystyrene foam. Figure 3b shows a visible camera image. The raw range image with flame environment noise and the processed image are shown in Figs. 3(c) and 3(d) respectively. Although the range image including the noise caused by flames is not so degraded, this noise can be decreased considerably by an accumulative averaging process if the observed targets remain still for a few seconds. The processed images are sufficiently clear to enable recognition of the environment around the robot.

1. A. V. Jelain, IEEE Spectrum **18**, 46 (1981).
2. T. Kami, and Y. Kumano, J. Jpn. Soc. of Fire Disaster **28**, 7 (1978).
3. M. Kimura, O. Yamada, H. Takahashi, and H. Naitoh, J. Rob. Mech. **1**, 274 (1989).

Thursday
May 16, 1991
Convention Center Room 310

Afternoon
CThL

1:00 pm Guided Wave Lasers

Clifford R. Pollock, *Cornell University, Presider*

1:00 pm

Diode-pumped, ion-implanted crystal waveguide lasers

S. J. Field, D. C. Hanna,* D. P. Shepherd,* A. C. Tropper,* P. J. Chandler,† P. D. Townsend,† and L. Zhang†
Department of Physics, University of Southampton, Southampton SO9 5NH, UK

We have recently reported the use of ion-implantation to form planar waveguide lasers in Nd:YAG crystals.[1,2] Here, for the first time, we report diode pumped operation using a 500 mW diode array. We also describe the use of ion implantation to form planar waveguide lasers in Nd:YAP and Nd:MgO:$LiNbO_3$.

Implanting He^+ ions, with energies of a few MeV, through the polished surface of a dielectric material produces controllable refractive index changes in the top few microns. Different crystals have different responses to ion-implantation, but in general waveguides can be produced by the formation of a low refractive index barrier (Fig. 1(a)), or by a refractive index increase in the guide region (Fig. 1(b)). Planar waveguide lasers have been made with both types of refractive index profile.

The geometry of a planar waveguide allows efficient coupling of a diode array pump laser. Using undoped ion-implanted waveguides, we obtained launch efficiencies of >50%. With the (line) focusing arrangement (Fig. 2) thresholds as low as ~8 mW absorbed power were obtained for a 16 μm by 2 μm spot size focus (1/e FWHM at the input of the waveguide) in Nd:YAG. The production of channel waveguides is currently in progress, and should lead to greatly reduced threshold values. Using a 16% output coupler slope, efficiencies of ~17% (with respect to absorbed power) were obtained, giving maximum observed output powers of ~19 mW.

In addition, we demonstrated the first waveguide laser in Nd:YAP. A waveguide laser in proton exchanged Nd:MgO:$LiNbO_3$ was previously demonstrated,[3] and we now show that an ion-implanted Nd:MgO:$LiNbO_3$ waveguide laser can also be successfully operated. Channel waveguides formed in YAP crystals could lead to low threshold upconversion lasers,[4] whereas $LiNbO_3$ is of interest due to its non-linear and electro-optic properties which, combined with a planar or channel waveguide structure, offers the possibility of many interesting devices.[5] For instance, the use of temperature-tuned 90° phase-matching to produce self-frequency doubling in a (diode-pumped) channel waveguide laser should lead to a very simple and efficient device.

Current and future work is aimed at extending these techniques to low threshold (diode pumped) operation of highly tunable sources. Promising waveguide structures have already been obtained in crystals such as sapphire, alexandrite, GGG, and $ZnWO_4$ using the ion implantation technique.

*Also with the Opto-electronics Research Centre, University of Southampton.
†School of Mathematical and Physical Sciences, University of Sussex, Falmer, Brighton BN1 9QH, UK

1. P. J. Chandler, S. J. Field, D. C. Hanna, D. P Shepherd, P. D. Townsend, A. C. Tropper, and L. Zhang. Electron. Lett. **25**, 985 (1989).
2. S. J. Field, D. C. Hanna, D. P. Shepherd, A. C. Tropper, P. J. Chandler, P. D. Townsend and L. Zhang, to be published IEEE J. Quantum Electron.
3. E. Lallier, J. P. Pochelle, M. Papuchon, C. Grezes-Besset, E. Pelletier, M. de Micheli, M. Li, Q. He, and D. B. Ostrowsky, Electron. Lett. **25**, 1491 (1989).
4. A. J. Silversmith, W. Lenth, and R. M. Macfarlane, Appl. Phys. Lett. **51**, 1977 (1987).
5. T. Y. Fan, A. Cordova-Plaza, M. J. F. Digonnet, R. L. Byer, and H. J. Shaw, J. Opt. Soc. Am. **3**, 140 (1986).

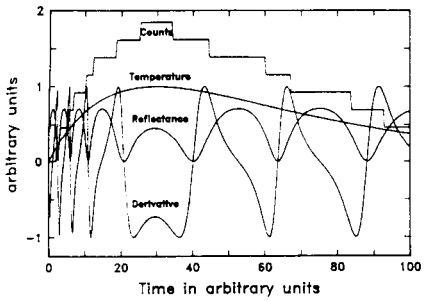

ThK3 Fig. 3. Simulation results showing the ..fer temperature, the reflected signal, the differ-..ntial signal, and number of counts as a function ..r time during thermal cycling. Each count registered corresponds to a temperature change of 1.2 of an optical fringe, or about 3.1°C for a 640-μm-thick silicon wafer.

	$0 \le \frac{(R' - R'_{min})}{(R'_{max} - R'_{min})} < 0.1$	$0 \le \frac{(R'_{max} - R')}{(R'_{max} - R'_{min})} < 0.1$
$dR/dt > 0$	+	−
$dR/dt < 0$	−	+

CThK3 Table 1. The sign of the counts generated during thermal cycling when $R \simeq R_{av}$. A "+" ("−") sign corresponds to increasing (decreasing) temperature.

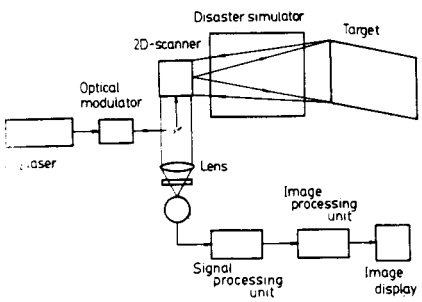

CThK4 Fig. 1. Block diagram of laser vision sensor.

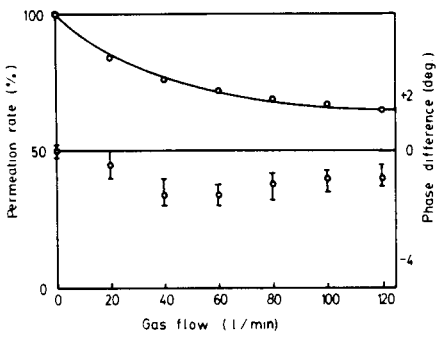

CThK4 Fig. 2. Example of laser propagation characteristics in a flame environment.

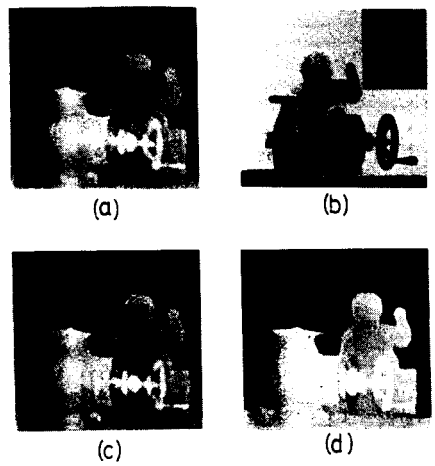

CThK4 Fig. 3. Target images: (a) range image in an indoor environment; (b) visible camera image; (c) range image with noise from a flame environment; and (d) range image processed by accumulative averaging process.

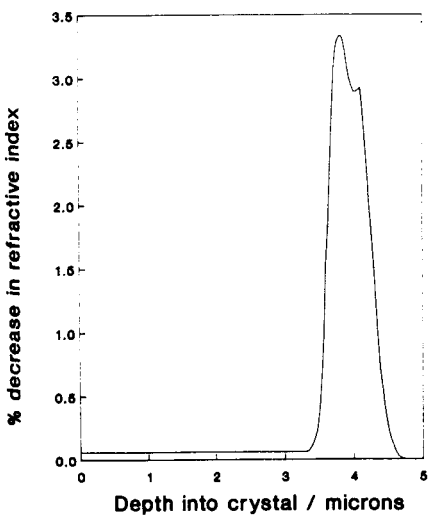

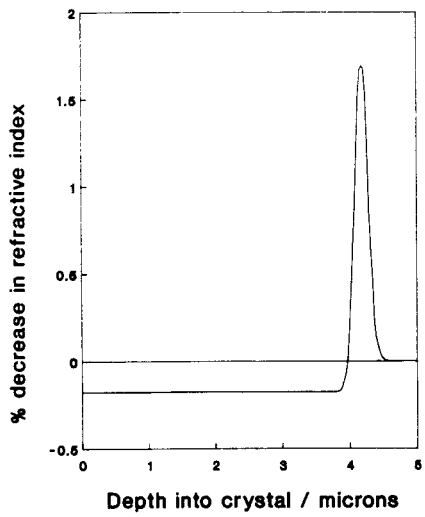

CThL1 Fig. 1. Waveguide Refractive Index Profiles (a) Low index barrier guide, e.g., Nd:YAP, (b) Index enhancement guide, e.g., Nd:YAG

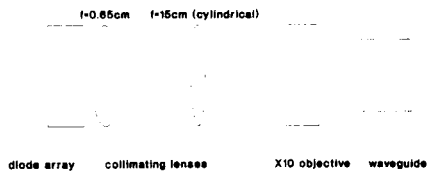

CThL1 Fig. 2. Focussing arrangement for diode array pumping.